

Fast and fully-automated multi-criterial treatment planning for adaptive HDR brachytherapy for locally advanced cervical cancer

Oud, Michelle; Kolkman-Deurloo, Inger Karine; Mens, Jan Willem; Lathouwers, Danny; Perkó, Zoltán; Heijmen, Ben; Breedveld, Sebastiaan

DOI

[10.1016/j.radonc.2020.04.017](https://doi.org/10.1016/j.radonc.2020.04.017)

Publication date

2020

Document Version

Final published version

Published in

Radiotherapy and Oncology

Citation (APA)

Oud, M., Kolkman-Deurloo, I. K., Mens, J. W., Lathouwers, D., Perkó, Z., Heijmen, B., & Breedveld, S. (2020). Fast and fully-automated multi-criterial treatment planning for adaptive HDR brachytherapy for locally advanced cervical cancer. *Radiotherapy and Oncology*, 148, 143-150. <https://doi.org/10.1016/j.radonc.2020.04.017>

Important note

To cite this publication, please use the final published version (if applicable). Please check the document version above.

Copyright

Other than for strictly personal use, it is not permitted to download, forward or distribute the text or part of it, without the consent of the author(s) and/or copyright holder(s), unless the work is under an open content license such as Creative Commons.

Takedown policy

Please contact us and provide details if you believe this document breaches copyrights. We will remove access to the work immediately and investigate your claim.



Original Article

Fast and fully-automated multi-criterial treatment planning for adaptive HDR brachytherapy for locally advanced cervical cancer

Michelle Oud^{a,b,*}, Inger-Karine Kolkman-Deurloo^a, Jan-Willem Mens^a, Danny Lathouwers^b, Zoltán Perkó^b, Ben Heijmen^a, Sebastiaan Breedveld^a^aErasmus MC Cancer Institute, Department of Radiation Oncology, University Medical Center Rotterdam; and ^bDelft University of Technology, Faculty of Applied Sciences, Department of Radiation Science and Technology, The Netherlands

ARTICLE INFO

Article history:

Received 13 February 2020

Received in revised form 10 April 2020

Accepted 13 April 2020

Available online 20 April 2020

Keywords:

High-dose-rate brachytherapy

Cervical cancer

Multi-criteria optimization

Automated treatment planning

Adaptive treatment

Adaptive treatment planning

ABSTRACT

Purpose: To develop and evaluate a fast, automated multi-criterial treatment planning approach for adaptive high-dose-rate (HDR) intracavitary + interstitial brachytherapy (BT) for locally advanced cervical cancer.

Methods and materials: Twenty-two previously delivered single fraction MRI-based HDR treatment plans (SF_{clin}) were used to guide training of our in-house system for multi-criterial autoplanning, aiming for an autoplan quality superior to the training plans, while respecting the clinically desired “pear-shaped” dose distribution. Next, the configured algorithm was used to automatically generate treatment plans for 63 other fractions (SF_{auto}). The SF_{auto} plans were compared to the corresponding SF_{clin} plans in blind pairwise comparisons by an expert clinician. Then, the effect of adaptive autoplanning on total treatment (TT) plans (external beam + 3 BT fractions) was evaluated for 16 patients by simulating the clinically applied adaptive strategy to generate TT_{auto} plans and compare them with the corresponding clinical treatments (TT_{clin}).

Results: In the blind comparisons, all SF_{auto} plans were considered clinically acceptable. In 62/63 comparisons, SF_{auto} plans were considered at least as good as, or better than the corresponding SF_{clin} . The average optimization time for autoplanning was 20.5 ± 19.2 s (range 4.4–106.4 s) per plan. In 14 of 16 TT_{auto} plans, the desired total dose of 90 Gy (EQD₂) was obtained, compared to only 9 in the corresponding TT_{clin} , while autoplanning also decreased bladder and rectum doses.

Conclusions: Fast, fully-automated multi-criterial treatment planning for adaptive HDR-BT for locally advanced cervical cancer is feasible. Autoplans were superior to corresponding clinical plans.

© 2020 The Authors. Published by Elsevier B.V. Radiotherapy and Oncology 148 (2020) 143–150 This is an open access article under the CC BY license (<http://creativecommons.org/licenses/by/4.0/>).

Several systems for automated treatment planning for external beam radiotherapy (EBRT) have been developed, demonstrating consistent high plan quality, with automatically generated plans often being preferred over manually generated plans [1–12].

In recent years, several approaches for high-dose-rate (HDR) brachytherapy (BT) automated treatment planning (autoplanning) have been proposed. For prostate cancer HDR-BT, Maree et al. and Cui et al. [13,14] approximated the Pareto-front for plan selection, allowing the user to make the final trade-off. A user-independent approach was presented by Breedveld et al. [15], who developed a system for automated multi-criterial treatment planning for

prostate HDR-BT, based on their in-house, clinically applied autoplanning system for EBRT, and demonstrated superiority of automated treatment planning over conventional HDR-BT treatment planning.

A unique objective in locally advanced cervical cancer HDR-BT planning is to not only achieve adequate target coverage and acceptable organ-at-risk (OAR) doses, but to also realize this with a *pear-shaped* dose distribution. For cervical cancer HDR-BT autoplanning, Lessard et al. [16] proposed a dose-based objective function in which the weighted sum over the high-risk clinical target volume (CTV_{HR}), a manually contoured pear shape, and the OARs was optimized. The relative weights of the structures needed to be tuned per patient in order to achieve clinically favorable treatment plans. Hanania et al. [17] used tuned settings for the inverse planning algorithm from the TPS, but also required fine-tuning per patient. Guthier et al. [18] focused on target coverage maximization (weighted sum of CTV_{HR} and intermediate risk CTV) under dose-volume based constraints on the OARs. They did not explicitly

* Correspondence author at: Erasmus MC Cancer Institute, Department of Radiation Oncology, University Medical Center Rotterdam, PO Box 2040, 3000 CA, Rotterdam, The Netherlands.

E-mail addresses: m.oud@erasmusmc.nl (M. Oud), i.kolkman-deurloo@erasmusmc.nl (I.-K. Kolkman-Deurloo), j.w.m.mens@erasmusmc.nl (J.-W. Mens), d.lathouwers@tudelft.nl (D. Lathouwers), z.perko@tudelft.nl (Z. Perkó), b.heijmen@erasmusmc.nl (B. Heijmen), s.breedveld@erasmusmc.nl (S. Breedveld).

address other aims such as generating a pear-shaped dose distribution, and minimizing OAR dose. A way to avoid manual tuning for cervical cancer HDR-BT is presented by Shen et al. [19], who used deep reinforcement learning to mimic actions of a manual planner by predicting suitable weight adjustments. The optimization problem consisted of constraints on the CTV_{HR} and an artificial pear-shape, while the dose to the OARs was minimized by using a weighted-sum function. There was no explicit steering on trade-offs between the dose in the target and OARs and there were no constraints on the dose to the OARs.

In this study, we follow the work by Breedveld et al. [15] to develop an approach for fully automated treatment planning for cervical cancer HDR-BT. Hereto, the autoplanning system was adapted for combined intracavitary + interstitial (IC + IS) HDR-BT for locally advanced cervical cancer. Two studies for autoplanning validation were conducted: (1) blind clinician comparisons of single fraction autoplans (SF_{auto}) with their corresponding clinical plans (SF_{clin}), and (2) comparisons of cumulative, total treatment (TT; EBRT + 3 BT fractions) dose distributions generated with adaptive autoplanning of the three BT fractions (TT_{auto}), with corresponding clinically delivered adaptive plans (TT_{clin}).

Methods and materials

Patients

The patients in this study were treated between 2015 and 2018 for stage 2.B-4.A cervical cancer. Treatment consisted of EBRT (23 fractions of 2 Gy or 25–27 fractions of 1.8 Gy) and BT (three or four fractions spread over three weeks). Patients were treated using the Utrecht applicator (Elekta AB, Stockholm, Sweden) with up to 10 interstitial needles. In each BT fraction, after applicator implantation an MRI or CT was obtained for adaptive planning.

For this study, only MRI-based fractions were considered because they were fully contoured (CTV_{HR} + OARs), resulting in a database with MRIs and corresponding clinical dose distributions of 85 fractions belonging to 34 patients. The average CTV_{HR} volume was $29.4 \pm 12.5 \text{ cm}^3$ (range 8.5–92.0 cm^3). In 56 fractions interstitial needles were implanted (average 4.4 ± 2.4 needles). A subset of 48 fractions belonged to 16 patients with an MRI in all three BT sessions available for this study. The remaining 37 plans belonged to 18 patients for whom one or more fractions were not selected because they were CT-based, or problems occurred when retrieving the data.

Clinical planning

State-of-the-art clinical treatment planning [20] was performed manually in our clinical treatment planning system Oncentra-Brachy (version 4.5.1, Elekta AB, Stockholm, Sweden), using delineated scans with a reconstructed applicator, while considering already delivered EBRT and BT dose.

An overview of the clinical planning aims as used between 2015 and 2018 at our institution is provided in Table 1. Limits and goals for the dosimetric parameters are defined for total treatments (TT: EBRT + BT) and presented as equivalent doses of 2 Gy per fraction (EQD_2). The dose received during EBRT was assumed to be uniform. No deformable registration was applied before summing EBRT and BT dosimetric plan parameters [21].

The general goal at the start of BT treatment planning was to evenly distribute remaining OAR tolerance doses and the required additional CTV_{HR} dose amongst three or four fractions. However, in the first fractions higher OAR doses could be accepted if it was expected to be necessary to obtain the minimum CTV_{HR} dose of 85 Gy in the total treatment. The maximum OAR tolerances in the total treatments were however always respected.

Table 1

Overview of the clinical planning aims. Presented EQD_2 are for total treatments (TT), assuming $\alpha/\beta = 10 \text{ Gy}$ for the CTV_{HR} and $\alpha/\beta = 3 \text{ Gy}$ for OARs.

<i>Dosimetric criteria</i>			
Structure	Dosimetric measure	Limit for total EQD_2	Goal for total EQD_2
CTV_{HR}	$D_{90\%}$	85 Gy	>90 < 95 Gy
Bladder	D_{2cc}	90 Gy	<80 Gy
Rectum	D_{2cc}	75 Gy	<65 Gy
Sigmoid	D_{2cc}	75 Gy	<70 Gy
Small Bowel	D_{2cc}	75 Gy	<60 Gy
<i>Other objectives</i>			
Pear-shaped isodose lines around intracavitary applicator			
Minimal dosimetric contribution from needles relative to intracavitary applicator, preferably below 20%			
Smooth dose distribution: no steep dose gradients and no hot or cold spots within the intracavitary applicator			
After delivering >93.8 Gy to the CTV_{HR} , prioritize OAR sparing over increasing CTV_{HR} dose			
Prioritize small bowel sparing towards goal over sparing other OARs			

Clinical BT planning started from a standard normalized treatment plan, in which the dwell positions in the intracavitary part of the applicator were evenly active. Dwell positions in the needles were then activated and dwell times in the standard plan were adjusted graphically by dragging isodose lines in the TPS. This process took 15–30 min per plan.

Automated planning

Erasmus-iCycle was used as a basis for automated plan generation [10,11,15]. The system uses a so-called ‘wish-list’ to steer the multi-criterial optimization. The wish-list contains hard planning constraints and prioritized objectives, and defines the lexicographic plan generation. A well-tuned wish-list results in clinically acceptable treatment plans with favorable trade-offs between the treatment objectives. The treatment site specific wish-lists are constructed in an iterative tuning process in close collaboration with the expert clinicians, using repetitive autoplanning, plan evaluation and wish-list adjustments for a small set of training patients (Electronic appendix of [11]).

Wish-list

The wish-list used for autoplanning in this study (Table 2) was configured with an expert clinician (Dr. Jan-Willem Mens, JWM), in line with clinical planning. Twenty-two of the 85 available treatment fraction MRIs with corresponding clinical dose distributions were used for training. Training fractions were selected to cover the full range of CTV_{HR} volumes. Because of the adaptive planning, the wish-list contains fraction-specific dosimetric parameters. All activated dwell positions (IC + IS) were available during automatic optimizations.

In line with the clinical protocol (Table 1), the final wish-list contained hard constraints for the D_{2cc} of the OARs (bladder, rectum, sigmoid and small bowel). The DVH-based cost-functions in the wish-list were implemented similar to the approach presented in [15]. To constrain the dwell time modulation and enforce smooth dose distributions, a quadratic cost-function which penalizes the second derivative of the dwell times of adjacent dwell positions in the intracavitary applicator, was used as constraint, similar to fluence map smoothing in EBRT [22]. The dose in the CTV_{HR} was optimized in three steps (priorities 1, 5 and 7 in Table 2). A pear-shaped dose distribution was created by optimizing on two artificially created structures (‘pear’ and ‘pear-inside’) which follow the dwell positions in the tandem and ovoids of the applicator

Table 2

Wish-list for per-fraction autoplanning for HDR-BT for cervical cancer, and total cumulative treatment aims for EBRT + 3BT (last column). Per-fraction parameters (L_j^i dose limit for structure i in fraction j , and $G_j^{i,p}$ dose goal for structure i in priority p and fraction j) in the wish-list were patient-specific and related to the performed adaptive planning (Section “Clinical planning”). N equals the number of needles. All doses are presented in EQD₂. The arrows indicate whether the objective was minimized (down) or maximized (up).

Constraints per fraction				
	Structure i	Constraint function	Dose limit in fraction j, L_j^i	Cumulative dose limit $L_{cum}^i = (EQD_2)_{EBRT}^i + \sum_j L_j^i$
	Bladder (B)	D_{2cc}	L_j^B Gy	90 Gy
	Rectum (R)	D_{2cc}	L_j^R Gy	75 Gy
	Sigmoid (S)	D_{2cc}	L_j^S Gy	75 Gy
	Small Bowel (SB)	D_{2cc}	L_j^{SB} Gy	75 Gy
	Intracavitary dwell positions	Quadratic function	Dwell time modulation $<24^* \text{ s/mm}^2$	
Objectives per fraction				
Priority p	Structure i	Objective in fraction j	Goal for fraction j	Cumulative dose goal $G_{cum}^i = (EQD_2)_{EBRT}^i + \sum_j G_j^{i,p}$
1	CTV _{HR} (T)	$\uparrow V_{G_j^{T,1}} \text{ Gy}$	90%	$D_{90\%} > 90 \text{ Gy}$
2	Pear	$\uparrow V_{5.9^*} \text{ Gy}$	96%	
3	Pear Inside	\uparrow Quadratic underdose (penalize $D < 8^* \text{ Gy}$)	0.1^* Gy^2	
4	Needles	$\downarrow \tau_{needles}(\text{Eq (1)})$	$0.1 + 0.015 N^*$, sufficient if $\frac{1}{2}(0.1 + 0.015 N)^*$	
5	CTV _{HR}	$\uparrow V_{G_j^{T,5}} \text{ Gy}$	90%	$D_{90\%} > 93.8 \text{ Gy}$
6	Bladder	$\downarrow V_{G_j^{B,6}} \text{ Gy}$	2 cc	$D_{2cc} < 80 \text{ Gy}$
6	Rectum	$\downarrow V_{G_j^{R,6}} \text{ Gy}$	2 cc	$D_{2cc} < 65 \text{ Gy}$
6	Sigmoid	$\downarrow V_{G_j^{S,6}} \text{ Gy}$	2 cc	$D_{2cc} < 70 \text{ Gy}$
6, weight 4*	Small Bowel	$\downarrow V_{G_j^{SB,6}} \text{ Gy}$	2 cc	$D_{2cc} > 65 \text{ Gy}$
7	CTV _{HR}	$\uparrow V_{G_j^{T,7}} \text{ Gy}$	90%	$D_{90\%} > 95 \text{ Gy}$

* Parameters indicated with an asterisk were chosen empirically based on training plans and were tweaked in collaboration with the expert clinician.

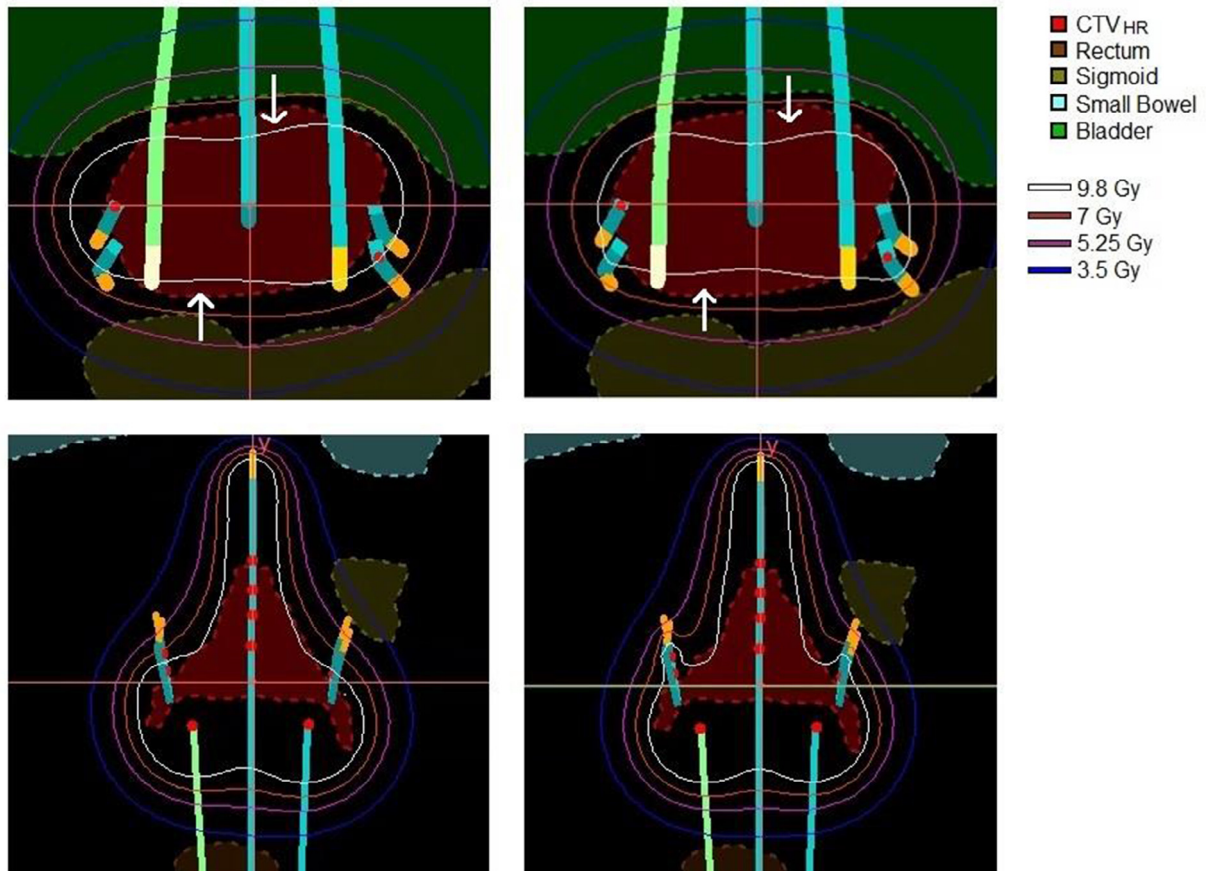


Fig. 1. Automatically generated dose distribution (left) and clinical dose distribution (right) with projected applicator for a single fraction for an example patient in the applicator coordinate system. The top slices (plane perpendicular to the intra uterine tube) demonstrate improved CTV_{HR} coverage for a reference dose of 9.8 Gy in the automatically generated dose distribution. The white arrows indicate positions of improved coverage. The bottom slices (plane parallel to the intra uterine tube) show the pear-shaped dose distribution. The shown isodose lines represent the physical doses.

at distances of 9 mm and 5 mm respectively, excluding overlap areas with the target or OARs (priorities 2 and 3). The 4th priority in the wish-list aims at reducing the relative dose contribution from the needles using $\tau_{needles}$ as defined by:

$$\tau_{needles} = \frac{t_{needles}}{t_{total}} \quad (1)$$

where t_{total} represents the total accumulated dwell time for all dwell positions (IC + IS) and $t_{needles}$ the total dwell time for only the interstitial part of the implant. The goal value was related to the number of available needles N (Table 2). The priority 6 objective aims at reducing OAR dose, where dose reduction in the small bowel was considered more relevant than other OARs and was thus assigned a relative weighting factor of 4.

Blind comparisons of single fraction autoplans (SF_{auto}) and clinical plans (SF_{clin})

To enable fair comparisons between SF_{auto} and SF_{clin} plans, the fraction-specific parameters L_j^i and $G_j^{i,p}$ in Table 2 were based on the constraints and goals used for the corresponding SF_{clin} . In this way, plans based on the same treatment goals could be compared, the only difference being the way of plan generation, manually or automated.

Comparison of total treatment adaptive autoplans (TT_{auto}) with clinical plans (TT_{clin})

For the TT comparisons, an automated adaptive strategy was simulated, in line with clinical practice (Section “Clinical planning”). To compute L_j^i and $G_j^{i,p}$, the total dose received up to this

fraction (EBRT and 0, 1 or 2 automatically generated BT fractions) was taken into account, while aiming at an equal spread of required or allowed dose to the CTV_{HR} and OARs over the remaining fractions. However, if the absolute minimum cumulative dose goal of 85 Gy (EQD₂) to the CTV_{HR} seemed to be infeasible, up to 5% more dose than L_j^i was allowed to the OARs in the first fraction and up to 3% in the second fraction. In the third and final fraction, the maximum tolerances (Table 1) were always respected.

Optimization details

The dose optimization points (voxels) were sampled with a density of 300 voxels/cc for all structures. To speed up computations, only the parts of the OARs within a 35 mm radius from the dwell positions were taken into account during optimizations. Beyond this distance, the maximum expected dose is anyway much less than the constrained values, which was verified by visual inspection for the training patients and had no impact on the resulting plan. Both the dose-volume cost-functions and the relative needle contribution cost-function (Eq. (1)) are non-convex. We used our in-house developed interior-point solver with extended functionality for non-convex optimization for these functions, see [23,15]. The optimizations were performed on an Intel Core i7-7700 with 4 cores running at 3.6 GHz. After optimization in Erasmus-iCycle, the dwell-times were imported in the clinical TPS for final dose calculation and comparisons with clinical plans.

Validation of automated planning

First, blind comparisons of single fraction autoplans (SF_{auto}) with corresponding clinical plans (SF_{clin}) were performed for the

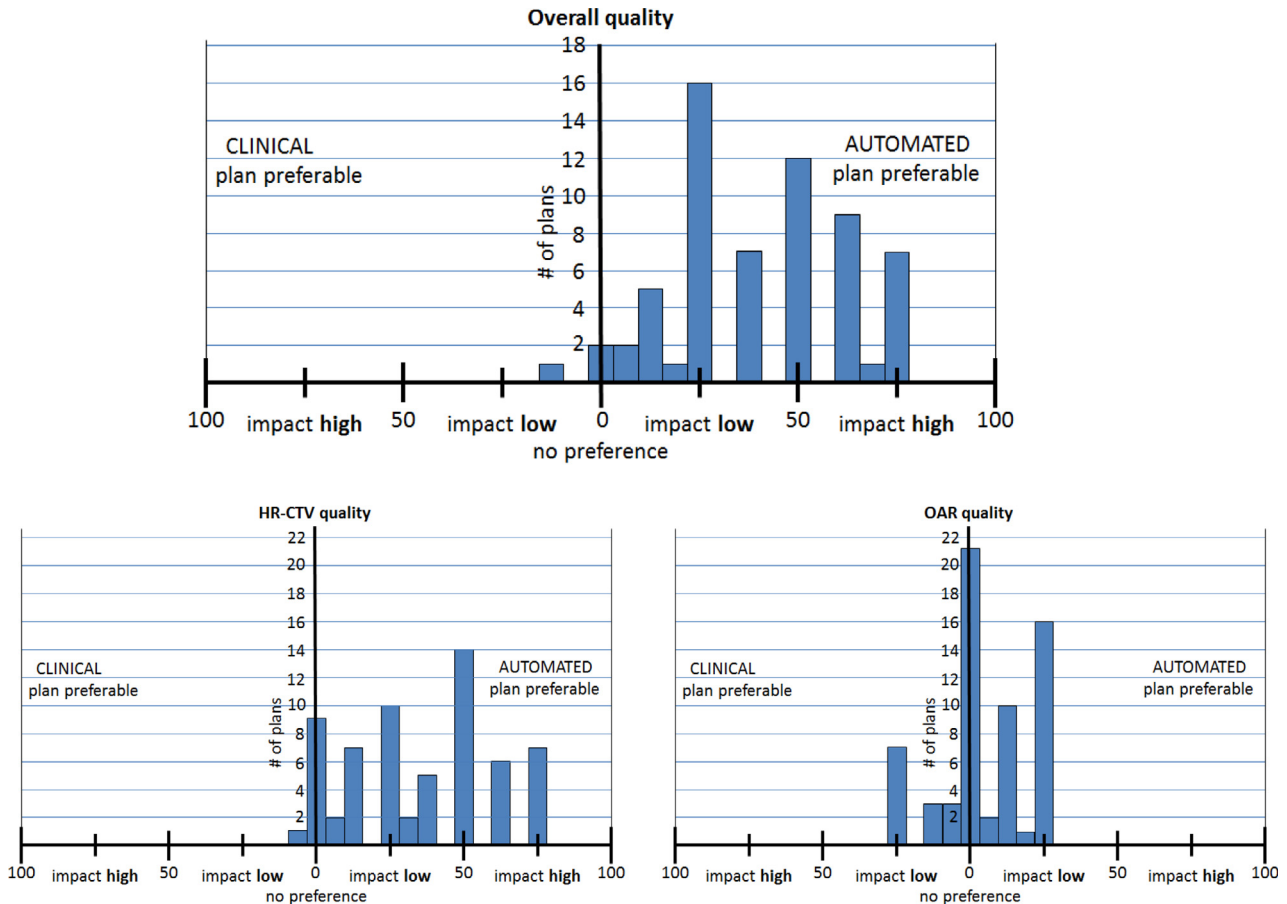


Fig. 2. Histograms showing results of the 63 clinician's blind comparisons of a single fraction autoplan with the corresponding clinically delivered plan. The x-axis shows the clinician's visual analog scale scores (Appendix A).

63 SF_{clin} plans that were not used in wish-list tuning. The pairwise plan comparisons were performed in the clinical TPS by an expert clinician (JWM), using the 3D dose distributions and DVH parameters of these plans, while considering also DVH parameters of previous BT fractions and the EBRT course, that were also provided. There were no pre-defined criteria for the comparisons; the clinician followed his routine workflow for plan evaluation. The clinician first assessed the clinical acceptability of both plans, followed by assessments of differences in (i) overall quality, (ii) CTV_{HR} dose and (iii) OAR dose, using a visual analog scale (Appendix A).

Second, total treatment adaptive autoplans (TT_{auto}) were compared with the clinical plans (TT_{clin}) for the 16 patients with an MRI in each BT fraction. Pairwise differences in the dosimetric plan parameters listed in Table 1 were assessed in the clinical TPS. After importing the dwell-times of the autoplans in the clinical TPS, the DVH parameters did not exactly match the Erasmus-iCycle optimized ones due to small differences in the implementation of volume and dose-point definition between the two systems. Therefore, D_{90%} CTV_{HR} in the last TT_{auto} fraction could be rescaled up to 93.8 Gy if possible within OAR limits, or down to 95 Gy in case the D_{90%} of TT_{auto} exceeded 95 Gy. Statistical significance of differences in plan parameters was assessed with the paired Wilcoxon signed-rank test.

Results

Fig. 1 shows an example of an SF_{auto} plan, compared to the corresponding SF_{clin} plan, clearly showing the desired pear-shape in both dose distributions. All 63 SF_{auto} plans were considered clinically acceptable by the clinician, while 1 clinical plan was (in retrospect) not. The clinician's scores, presented in Fig. 2, demonstrate superiority for the automatically generated plans in terms of overall plan quality. In 60/63 cases SF_{auto} was preferred over SF_{clin}, in 2/63 cases the quality of the plans was considered equal (score = 0) and for 1/63 cases SF_{clin} was preferred over SF_{auto} because of a more favorable small bowel dose. The scoring for CTV_{HR} shows a similar trend with in 62/63 cases SF_{auto} similar or better than the clinical plan. For the OARs, the differences were less pronounced. Still, in 29/63 cases SF_{auto} was considered better, in 21/63 cases both plans were similar and for 13/63 cases SF_{clin} was preferred.

The average optimization time for the 63 SF_{auto} plans was 20.5 ± 19.2 s (range 4.4–106.4 s).

For the total treatment adaptive autoplans, the last fraction could be rescaled for 10/16 patients due to differences in TPSes to improve CTV_{HR} dose, with an average absolute difference in D_{90%} of 0.26 ± 0.21 Gy (range 0.10–0.80 Gy). Total treatment dosimetric parameters are compared in Fig. 3. The required minimum CTV_{HR} D_{90%} of 85 Gy (Table 1) was always obtained for TT_{auto}, whereas for two TT_{clin} plans it was not. Consequently, these two clinically delivered treatments did not strictly adhere to the requirements for clinical acceptability. This was due to an unfavorable anatomy of these patients, making manual treatment planning challenging. The first goal for the CTV_{HR} was to achieve a minimum dose of 90 Gy. This was obtained in 14/16 TT_{auto} plans, compared to 9/16 TT_{clin} plans. For all 16 patients the CTV_{HR} D_{90%} was highest in the TT_{auto} plan. This improvement was statistically significant ($p = 0.0004$) and clinically relevant with a mean D_{90%} for the TT_{auto} plans of 93.0 ± 2.0 Gy compared to 89.4 ± 3.2 Gy for TT_{clin}, with differences ranging from +1.4 to +6.0 Gy.

For the D_{2cc} of the OARs for the total treatment adaptive plans, the prescribed limits (Table 1) were never exceeded, neither for TT_{auto}, nor for TT_{clin} (Fig. 3). The dose in the bladder was significantly reduced in the TT_{auto} plans compared to TT_{clin} ($p = 0.05$) with

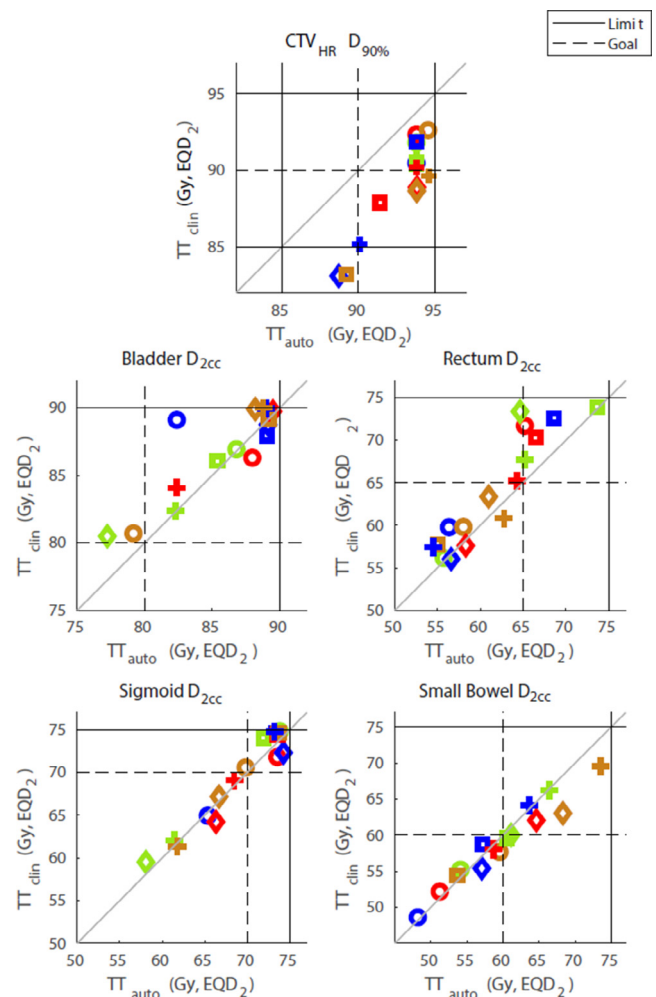


Fig. 3. Scatter plots showing CTV_{HR} D_{90%}, and bladder, rectum, sigmoid and small bowel D_{2cc} for the automatically generated and clinical total treatment plans (TT_{auto} and TT_{clin}). Each patient has her own colored symbol. Improvements in CTV_{HR} D_{90%} for TT_{auto} plans, and bladder and rectum D_{2cc} were statistically significant. There were no significant differences for the sigmoid and small bowel.

a mean reduction of 0.87 Gy (range −1.8 to 6.6 Gy). The rectum was also significantly more spared ($p = 0.04$), with a mean reduction in D_{2cc} of 1.4 Gy (range −4.9 to 6.3 Gy). There were no significant differences in D_{2cc} of the sigmoid ($p = 0.3$) and small bowel ($p = 0.3$).

Discussion

Optimization of the dose distribution for locally advanced cervical cancer HDR-BT is a complex problem, due to the special requirements of the dose distribution (pear-shaped), delivery restrictions (contributions by needles) and the adaptive treatment schedule. To the best of our knowledge, we have presented the first automated multi-criterial treatment planning solution considering each of the complexities, and capable of generating clinically favorable dose distributions. In the blind comparisons, all 63 single fraction autoplans were considered clinically acceptable by the expert clinician, and 62 of the 63 autoplans were scored similar or better than the clinically delivered plans.

In this study, we also proposed an adaptive treatment approach with a quantitative recipe for setting all fraction-specific treatment goals, depending on previously delivered doses. This adaptive

autoplanning approach was in line with the (somewhat less rigidly defined) clinical adaptive planning. Adaptive autoplanning was compared with clinical planning based on cumulative total treatment doses, as there exists no clinical scenario for comparisons of single fraction doses in adaptive treatment. Nonetheless, all single fraction autoplans fulfilled the clinical requirements (Table 1). The proposed procedure with adaptive single fraction autoplanning resulted in overall higher quality of total treatment dose distributions compared to clinical total dose. For all 16 patients, the $CTV_{HR} D_{90\%}$ was highest with automated planning. The number of patients who reached the desired minimum CTV_{HR} dose increased from 9/16 in the clinical treatment to 14/16 when using automated treatment planning.

With an average optimization time of 20.5 s per fraction, this approach shortens treatment planning times considerably, which are currently between 15 and 30 min in clinical practice.

The wish-list in this study was tailored to the treatment planning procedure at the Erasmus MC at the time of the treatment of the patients. The Erasmus MC has recently made the transition to the Embrace II protocol¹. As most challenging requirements in this protocol are similar to those for the current HDR-BT cervix plans, it is expected that the current wish-list can be adapted to generate clinically preferable dose distributions for Embrace II as well. In addition to limits and goals for the $D_{90\%}$ of the HR-CTV and D_{2cc} of the OARs, the EMBRACE II protocol includes more goals, for example for the $D_{98\%}$ of the CTV_{HR} , intermediate-risk CTV and gross tumor volume. Because the Embrace II protocol contains more objectives compared to the protocol in this study, manual treatment planning becomes even more challenging and an automatic approach could become even more valuable. However, tuning the desired trade-offs between the different objectives will be more time-consuming.

In the future, our HDR-BT autoplanning approach could be extended with optimization of the interstitial needle configuration (positions and insertion depth) of the applicator, by simulating the 10 possible needle positions and including an objective to mini-

mize the number of used needles and their insertion depths in the wish-list. Needles could then be implanted based on an individualized and automatically generated treatment plan that is optimized both for the dwell times and number and position of needles.

In conclusion, this study demonstrated that fast, fully-automated multi-criterial treatment planning for locally advanced cervical cancer HDR-BT was feasible, based on a well-tuned, clinically relevant wish-list. Blind pairwise clinician comparisons of single fraction manual- and autoplans pointed at a strong preference for the autoplans. Cumulative total doses resulting from adaptive treatment were also favorable when generated with per-fraction autoplanning. With autoplanning, planning times reduced from the current 15–30 min to 20.5 s on average.

Disclosure

The Erasmus MC Cancer Institute has research collaborations with Elekta AB, Stockholm, Sweden, and Accuray Inc, Sunnyvale, USA. The Delft University of Technology—Radiation Science & Technology has research collaborations with Varian Medical Systems, Palo Alto, USA. The presented work was not sponsored by any of the above named companies.

Conflict of Interest

None declared.

Appendix A. Scoring sheet for the blind comparisons.

See Fig. A1.

¹ <https://www.embracestudy.dk>

Patient reference ID:

Scoring date/time:

Acceptability

LEFT plan acceptable

RIGHT plan acceptable

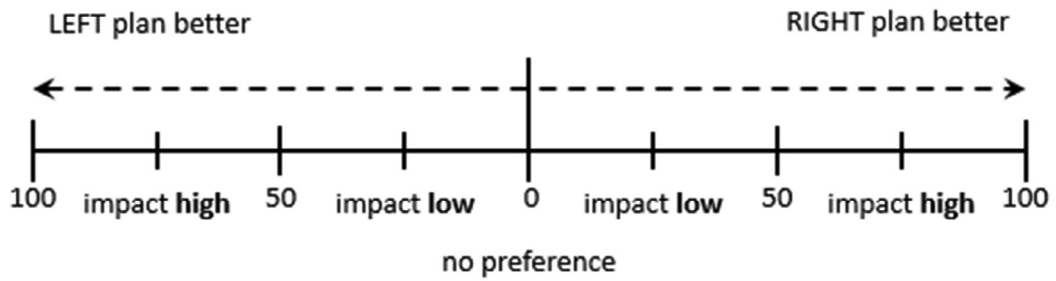
YES

NO

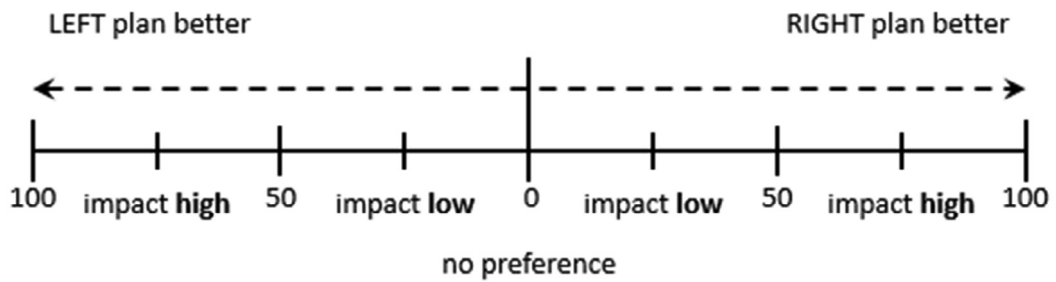
YES

NO

Overall plan quality



CTV quality



OAR quality

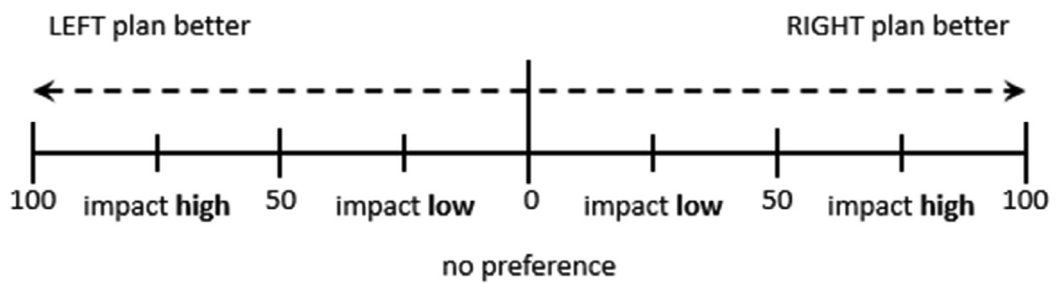


Fig. A1.

References

- [1] Hussein M, Heijmen BJ, Verellen D, Nisbet A. Automation in intensity modulated radiotherapy treatment planning—a review of recent innovations. *Br J Radiol* 2018;91:20180270. <https://doi.org/10.1259/bjr.20180270>.
- [2] Fogliata A, Belosi F, Clivio A, Navarria P, Nicolini G, Scorsetti M, et al. On the preclinical validation of a commercial modelbased optimisation engine: Application to volumetric modulated arc therapy for patients with lung or prostate cancer. *Radiother Oncol* 2014;113:385–91. <https://doi.org/10.1016/j.radonc.2014.11.009>.
- [3] Tol JP, Delaney AR, Dachele M, Slotman BJ, Verbakel WFAR. Evaluation of a knowledge-based planning solution for head and neck cancer. *Int J Radiat Oncol Biol Phys* 2015;91:612–20. <https://doi.org/10.1016/j.ijrobp.2014.11.014>.
- [4] Hussein M, South CP, Barry MA, Adams EJ, Jordan TJ, Stewart AJ, et al. Clinical validation and benchmarking of knowledgebased IMRT and VMAT treatment planning in pelvic anatomy. *Radiother Oncol* 2016;120:473–9. <https://doi.org/10.1016/j.radonc.2016.06.022>.
- [5] Hansen CR, Bertelsen A, Hazell I, Zukauskaitė R, Gyldenkerne N, Johansen J, et al. Automatic treatment planning improves the clinical quality of head and neck cancer treatment plans. *Clin Transl Radiat Oncol* 2016;1:2–8. <https://doi.org/10.1016/j.ctro.2016.08.001>.
- [6] Hansen CR, Nielsen M, Bertelsen AS, Hazell I, Holtved E, Zukauskaitė R, et al. Automatic treatment planning facilitates fast generation of high-quality treatment plans for esophageal cancer. *Acta Oncol* 2017;56:1495–500. <https://doi.org/10.1080/0284186X.2017.1349928>.
- [7] Marrasso L, Meattini I, Arilli C, Calusi S, Casati M, Talamonti C, et al. Auto-planning for VMAT accelerated partial breast irradiation. *Radiother Oncol* 2019;132:85–92. <https://doi.org/10.1016/j.radonc.2018.11.006>.
- [8] Purdie TG, Dinniwell RE, Fyles A, Sharpe MB. Automation and intensity modulated radiation therapy for individualized high quality tangent breast treatment plans. *Int J Radiat Oncol Biol Phys* 2014;90:688–95. <https://doi.org/10.1016/j.ijrobp.2014.06.056>.
- [9] Breedveld S, Storch PR, Heijmen BJ. The equivalence of multi-criteria methods for radiotherapy plan optimization. *Phys Med Biol* 2019;54:7199. <https://doi.org/10.1088/0031-9155/54/23/011>.
- [10] Breedveld S, Storch PR, Voet PW, Heijmen BJ. iCycle: Integrated, multicriterial beam angle, and profile optimization for generation of coplanar and noncoplanar IMRT plans. *Med Phys* 2012;39:951–63. <https://doi.org/10.1118/1.3676689>.
- [11] Heijmen BJ, Voet P, Fransen D, Penninkhof J, Milder M, Akhlat H, et al. Fully automated, multi-criterial planning for Volumetric Modulated Arc Therapy—An international multi-center validation for prostate cancer. *Radiother Oncol* 2018;128:343–8. <https://doi.org/10.1016/j.radonc.2018.06.023>.
- [12] Rossi L, Sharfo AW, Aluwini S, Dirkx M, Breedveld S, Heijmen BJ. First fully automated planning solution for robotic radiosurgery – comparison with automatically planned volumetric arc therapy for prostate cancer. *Acta Oncol* 2018;57:1490–8. <https://doi.org/10.1080/0284186X.2018.1479068>.
- [13] Maree SC, Luong NH, Kooreman ES, van Wieringen N, Bel A, Hinnen KA, et al. Evaluation of bi-objective treatment planning for high-dose-rate prostate brachytherapy—A retrospective observer study. *Brachytherapy* 2019;18:396–403. <https://doi.org/10.1016/j.brachy.2018.12.010>.
- [14] Cui S, Després P, Beaulieu L. A multi-criteria optimization approach for HDR prostate brachytherapy: II. Benchmark against clinical plans. *Phys Med Biol* 2018;63:. <https://doi.org/10.1088/1361-6560/aac24f205005>.
- [15] Breedveld S, Bennan AB, Aluwini S, Schaart DR, Kolkman-Deurloo IKK, Heijmen BJ. Fast automated multi-criteria planning for HDR brachytherapy explored for prostate cancer. *Phys Med Biol* 2019;64:. <https://doi.org/10.1088/1361-6560/ab44ff205002>.
- [16] Lessard E, Hsu IC, Pouliot J. Inverse planning for interstitial gynecologic template brachytherapy: truly anatomy-based planning. *Int J Radiat Oncol Biol Phys* 2002;54:1243–51. [https://doi.org/10.1016/S0360-3016\(02\)03802-6](https://doi.org/10.1016/S0360-3016(02)03802-6).
- [17] Hanania AN, Myers P, Yoder AK, Bulut A, Eraj S YuZH, Anderson ML, et al. Inversely and adaptively planned interstitial brachytherapy: A single implant approach. *Gynecol Oncol* 2019;152:353–60. <https://doi.org/10.1016/j.ygyno.2018.11.020>.
- [18] Guthrie CV, Damato AL, Viswanathan AN, Hesser JW, Crmack RAA. Fast multitarget inverse treatment planning strategy optimizing dosimetric measures for high-dose-rate (HDR) brachytherapy. *Med Phys* 2017;44:4452–62. <https://doi.org/10.1002/mp.12410>.
- [19] Shen C, Gonzalez Y, Klages P, Qin N, Jung H, Chen L, et al. Intelligent inverse treatment planning via deep reinforcement learning, a proof-of-principle study in high dose-rate Brachytherapy for cervical cancer. *Phys Med Biol* 2019;64:. <https://doi.org/10.1088/1361-6560/ab18bf115013>.
- [20] Nout RA, de Leeuw AAC, van Leeuwen RGH, Mans A, Verhoef CG, Jürgenliemk-Schulz IM. Implementatie en 'quality assurance' van 'state-of-the-art' radiotherapie voor gevorderd cervixcarcinoom in Nederland: een kwaliteitsbevorderingsproject. *Nederlands Tijdschrift voor Oncologie* 2017;14:117–21.
- [21] Swamidas J, Kirisits C, De Brabandere M, Hellebust TP, Siebert F-A, Tanderup K. Image registration, contour propagation and dose accumulation of external beam and brachytherapy in gynecological radiotherapy. *Radiother Oncol* 2020;143:1–11. <https://doi.org/10.1016/j.radonc.2019.08.023>.
- [22] Breedveld S, Storch P, Keijzer M, Heijmen B. Fast, multiple optimizations of quadratic dose objective functions. *IMRT Phys Med Biol* 2006;51:3569–79. <https://doi.org/10.1088/0031-9155/51/14/019>.
- [23] Breedveld S, van den Berg B, Heijmen B. An interior-point implementation developed and tuned for radiation therapy treatment planning. *Comput Optim Appl* 2017;68:209–42. <https://doi.org/10.1007/s10589-017-9919-4>.